

THE CHAOTIC BEHAVIOR OF THE LEAKY FAUCET

P. MARTIEN, S.C. POPE, P.L. SCOTT and R.S. SHAW

Board of Studies in Physics, University of California, Santa Cruz, CA 95064, USA

Received 28 August 1984; revised manuscript received 3 June 1985; accepted for publication 4 June 1985

A variety of phenomena associated with the chaotic behavior of a leaky faucet are displayed and discussed. Interpretations are suggested, both in terms of a simple one-dimensional analog simulation, and in terms of a Shannon-based information theory, in which a useful descriptive function, the *stored information*, is calculated from observed streams of data.

Several years ago Rössler suggested that the drips falling from a leaky faucet might provide a familiar example of a dynamical system capable of exhibiting chaotic behavior [1]. In the following, we report a summary of our experimental investigations to date on such a system. We find substantial evidence for a broad range of dynamical behavior, including period doubling, a transition to chaos, hysteresis, and a variety of complex behavior that remains as yet incompletely understood. We find that a mathematical model of a simple one-dimensional nonlinear oscillator may be used to simulate some of the simpler behavior of the leaky faucet, with good qualitative agreement. We also analyze the dynamical behavior in terms of a function we call the *stored information*, which quantifies our ability to predict future system states. Preliminary reports of these investigations have been presented previously [2]. Aspects of this work have also been described by two of us in undergraduate senior theses [3]. A lengthy paper providing additional description and analysis is available [4].

The basic apparatus is shown in fig. 1⁺¹. Distilled water, kept at a constant pressure head by means of a float valve (a modified Model A Ford carburetor) is allowed to flow through a needle valve to an orifice. Drips from the orifice interrupt the beam of a helium-neon laser directed onto a photocell; each of the resulting voltage pulses from the photocell is made to trigger the sweep of an oscilloscope, which provides a

gate pulse. The sequence of drips thus produces a stream of uniformly shaped pulses, one pulse per drip, which is fed to a Z80-based microcomputer⁺² for timing, storage and subsequent analysis. The microcomputer also is used to set the needle valve opening, through the use of a stepper motor coupled to the valve shaft, allowing the drip rate to be varied between about 30 drips per minute (the stable period 1 regime) and about 1200 drips per minute (just prior to the transition to smooth laminar flow). A typical data set, obtained at a single setting of the needle valve, consists of a few thousand pulses.

Although a complete description of the detailed behavior of the drips falling from an orifice requires a very large number of variables, we have chosen to focus our attention on a single, easily accessible variable, the time interval T_n between successive drips — the “drip interval”. A particularly revealing way to display the data from a single data set is to plot a map of T_{n+1} versus T_n . Fig. 2 shows a sequence of such plots, as the valve opening is set to increasingly larger values.

Simple periodic regimes such as the period-1 and period-2 attractors (figs. 2a, 2b) dominate the behavior of the leaky faucet at flow rates below about 200 drips/min. A period-doubling sequence leading to chaos appears to exist; the system is quiet enough to observe doubling up to period 4, or, with some imagination, period 8.

At drip rates ranging from about 200 drips/min to

⁺¹ Figure drawn by Chris Shaw.

⁺² The microcomputer was constructed by J.P. Crutchfield.

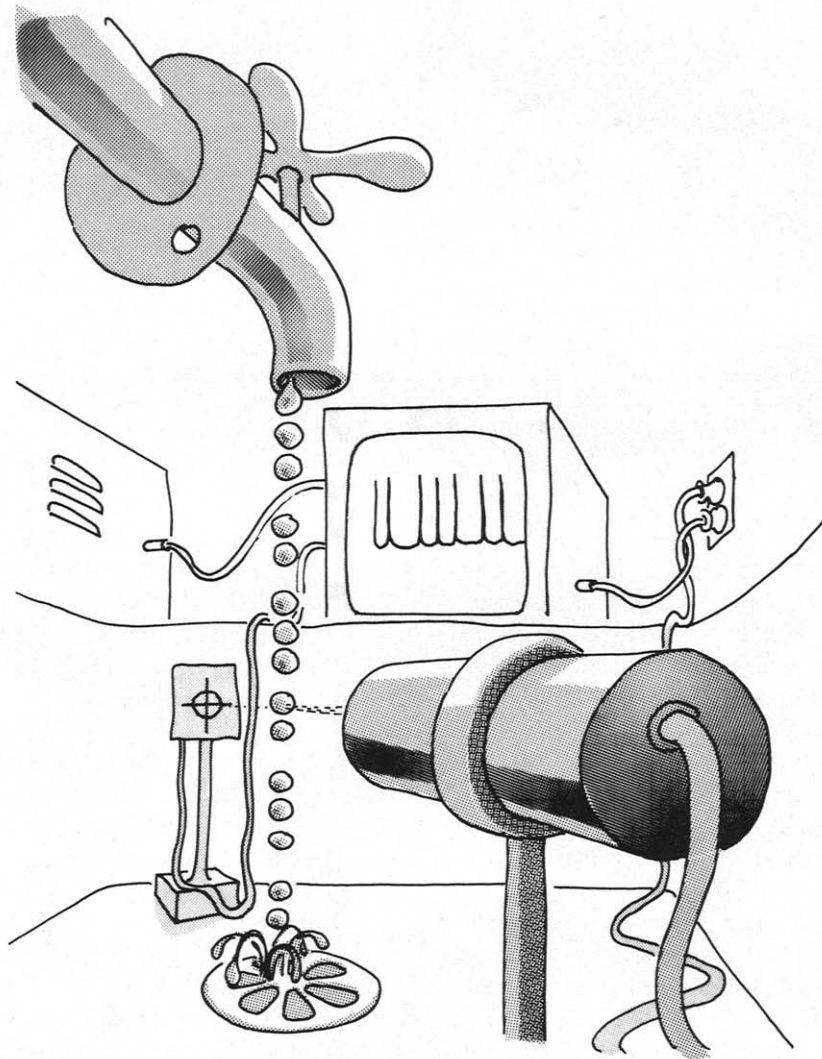


Fig. 1. A depiction of the experimental apparatus.

about 750 drips/min, “fuzzy humps” and “worms” predominate (figs. 2d–2f). These string-like, one-dimensional structures are often interspersed with simple periodic structures; fig. 2f shows such a string well on its way to becoming a period-3 attractor.

A wide variety of more complex structures are found at drip rates above 750 drips/min (figs. 2g–2i). At this point, the relative scatter of the measured periods, on the order of a few per cent for the previous attractors, increases dramatically to the order of fifty per cent. Accompanying this increase is a shift from

string-like structures to attractors with apparent dimension greater than one, and a sharp drop in the frequency of appearance of simple periodic attractors.

Two types of stability can be qualitatively distinguished. Stability against mechanical shock and random perturbations appears to be equally prevalent over the entire range of drip rates. However, the stability of given attractor structures in valve parameter space (the range of valve settings over which an attractor remains essentially unchanged) is much greater at the high flow rates.

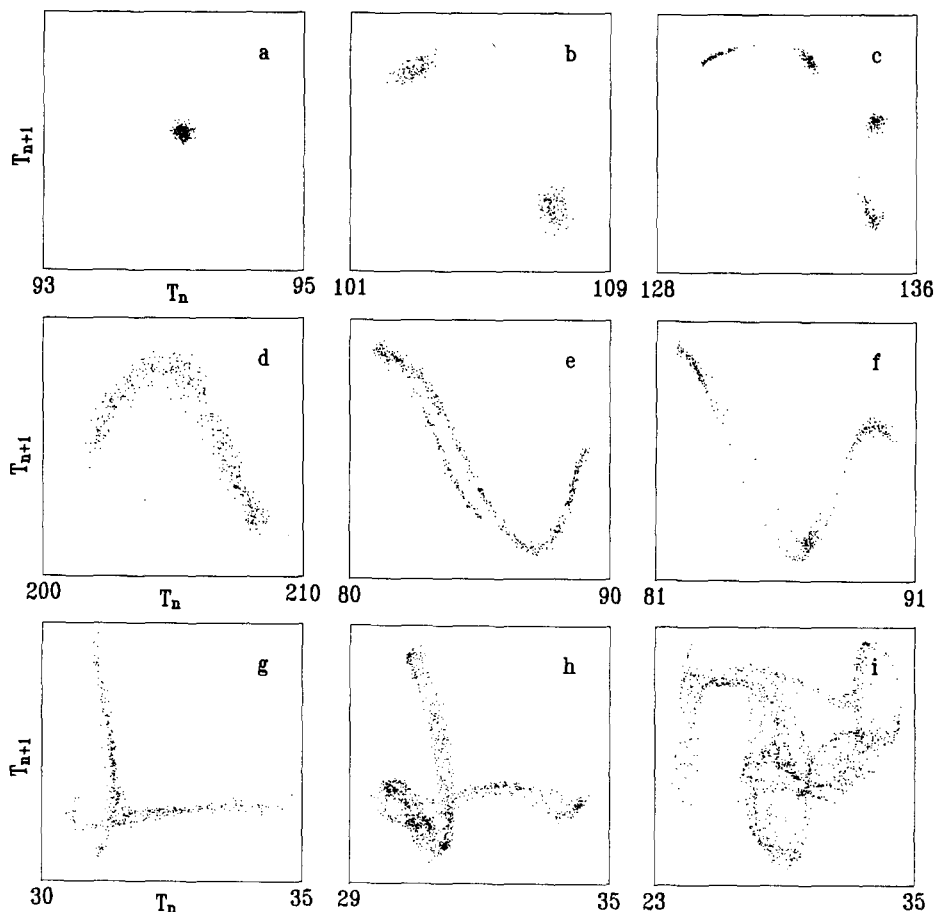


Fig. 2. Examples of T_{n+1} versus T_n return maps selected from the data. (a)–(c): Periodic behavior. (d)–(f): Low-dimensional chaotic behavior. (g)–(i): More complex chaotic behavior, appearing at higher flow rates. All time values are in milliseconds.

A mathematical model which simulates some of the behavior shown in fig. 2 may be developed as follows: A drop hanging from the orifice may oscillate, with a frequency that decreases as the drop mass increases. At a critical moment, which is sensitively dependent on the drop size and position, the drop will break away, setting the subsequent drop into a similar oscillation. This one-dimensional “mass-on-a-spring” type of oscillatory motion may be described by the following equation:

$$d(mv)/dt = mg - ky - bv, \quad (1)$$

where y is the position of the forming drop, $v = dy/dt$ is its velocity, m is its mass, and g , k and b are constant parameters. The mass is made to increase linearly with

time until the drop position exceeds a preset threshold. At this point, its valve is suddenly reduced by an amount proportional to the speed of the drop at that moment, thus simulating the breaking away of the drop. Fig. 3 shows data, in the form of T_{n+1} versus T_n maps, produced by an analog computer on which this equation is programmed. The behavior of the solutions to eq. (1) depends on at least four independent parameters (g , k , b and dm/dt), and we have not made a systematically exhaustive exploration of this behavior. However it is apparent that there exist regions of the parameter space for which this simple model produces solutions whose return maps are remarkably similar, in a qualitative sense, to those produced by the faucet when the flow rate is low enough (figs. 2a–2f). In

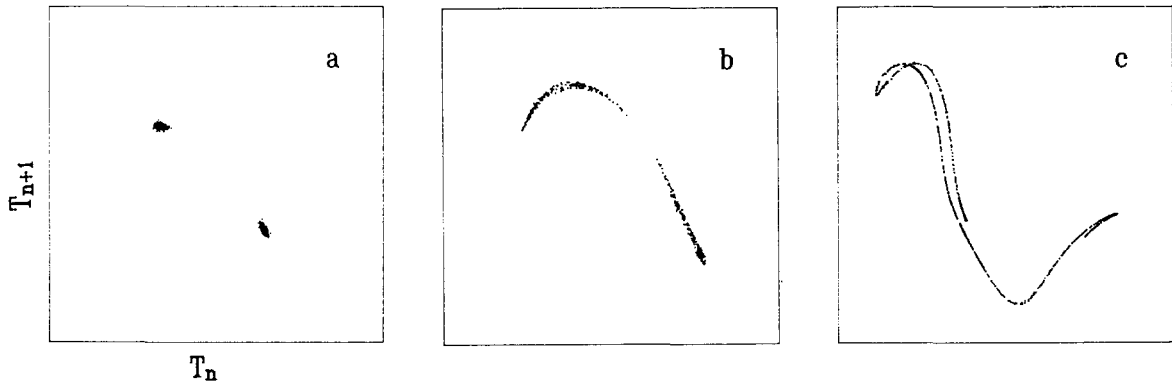


Fig. 3. T_{n+1} versus T_n return maps for the analog model, illustrating qualitative similarities with some of the attractor structures shown in fig. 2. Units of time are arbitrary, and thus are not shown.

particular we observe period-doubling bifurcations and low-dimensional chaotic motion for both systems.

Examination of the return maps of fig. 2 suggests the presence of noisy but well-defined attractors underlying the behavior of the system dynamics. For some systems, a description of the chaotic motion is aided by the determination of a "dimension" for some underlying attractor. For the leaky faucet, however, calculations of dimension have proven unsatisfactory, owing to the limited dynamic range of the data, the noise scale being almost as large as that of the prominent topological features.

Hence we have developed a new technique, in which we compute from a data set the function $I(t)$, the *stored information*. This function, which derives from Shannon's information theory [5], may in general be estimated from an observed data stream produced by any dynamical system using methods developed by one of the authors [4], and serves to provide a quantitative description of the system behavior. It is a measure of *predictability* in that it specifies how well we can predict the system's future state, given knowledge of its past behavior. We expect that $I(t)$ will be a decreasing function of time, as we become less able to predict behavior farther and farther into the future. Furthermore, $I(t)$ is an invariant under any arbitrary coordinate transformation of reasonable smoothness, a property allowing it to be estimated from data provided by any set of conveniently observed system variables. In particular, for the dripping faucet system, we may treat the easily

observed sequence of drip intervals as a valid data stream from which to estimate $I(t)$.

To be more precise, consider a data set consisting of a few thousand drip interval values T_1, T_2, T_3, \dots . The estimate of $I(t)$ is somewhat complicated by the fact that these drip intervals are embedded in continuous time, with the result that there may be a significant contribution to $I(t)$ from the *phase* of the drip pulse sequence. In what follows, to aid conceptual clarity, we start by ignoring this "phase information", to arrive at a function $I_1(t)$, the stored information associated with only the abstracted set of drip interval values. Subsequently we shall modify the calculation to include the phase variable.

We denote by \mathbf{T} a short sequence of a few adjacent measured intervals (often only one); we call this the *history vector*. T' represents a single future interval, separated by k intervals from the history, where $k = 1, 2, 3, \dots$. In this context, the stored information (in "bits") is given by

$$I_1(k) = \iint P_k(\mathbf{T}, T') \log_2 \left(\frac{P_k(\mathbf{T}, T')}{P(\mathbf{T})P(T')} \right) d\mathbf{T} dT'. \quad (2)$$

Here $P_k(\mathbf{T}, T') d\mathbf{T} dT'$ represents the joint probability that the history lies between \mathbf{T} and $\mathbf{T} + d\mathbf{T}$ and that the future interval lies between T' and $T' + dT'$. $P(\mathbf{T}) d\mathbf{T}$ is the unconditioned probability that the history vector lies between \mathbf{T} and $\mathbf{T} + d\mathbf{T}$, while $P(T') dT'$ is the similar probability that the future interval lies between T' and $T' + dT'$. We obtain an estimate of $I_1(k)$ from a data set through a binning procedure,

with the bin size less than the stochastic noise, to allow the above integral to be approximated by a sum. The relevant probabilities are estimated by counting occurrences of particular history vectors and future intervals. In our calculations, we include appropriate correction factors to remove bias arising from the binning procedure, resulting in a determination of $I_1(k)$ which is insensitive to bin size over a broad range. If the history vector consists of only a single interval T , then $P_k(T, T')$ is approximately equal to the density of points on a T_{n+k} versus T_n return map, while $P(T)$ and $P(T')$, which must be identical functions, are simply the projections of the return map point density onto each of the axes.

Now we proceed to include the additional contribution to the stored information involving knowledge of the phase. We denote by $I(k)$ the stored information which includes that associated with this additional phase variable, so that $I(k)$ serves to describe our ability to predict not only the magnitude of the future drip intervals, but also the probable times at which future drips will occur. If the drip intervals are fairly regular, that is, if the scatter of drip interval values is small compared with the average drip interval T_{av} , then the appropriate expression for $I(k)$ is given by

$$I(k) = \iiint P_k(T, S, T') \times \log_2 \left(\frac{T_{av} P_k(T, S, T')}{P(T)P(T')} \right) dT dS dT', \quad (3)$$

where T is the history vector, T' is the future interval separated by k intervals from the history, and S is the total intervening time between T and T' . Eq. (3) gives the stored information $I(t)$ for $t = kT_{av}$, where $k = 1, 2, 3, \dots$. With the observation of only the drip interval data, values of $I(t)$ calculated using eq. (3) represent lower bounds of information stored by the actual system. We do not give here complete derivations of eqs. (2) and (3). Further discussion of their applicability to our experimental results will be found in refs. [3,4].

There are two useful quantities associated with the stored information, which we call the *information storage capacity* and the *entropy generation rate*. The former is simply the maximum value of $I(k)$, namely $I(1)$. In the language of communication theory, this is the "channel rate", or "mutual information" between past and future system states [6]. The entropy genera-

tion rate is simply $I(1) - I(2)$, which may also be thought of as the initial rate of loss of predictability as future times are considered. This definition is equivalent to the Kolmogorov-Sinai entropy of noiseless, deterministic systems [7] in appropriate limits, but avoids the difficulties which arise in the definition of the deterministic entropy when a noise element is present. As with the stored information itself, both the information storage capacity and the entropy generation rate are geometric invariants.

Fig. 4 shows examples of both $I_1(k)$ and $I(k)$, estimated as described above, using the data of the "fuzzy hump" of fig. 2d, which occupies about 5 per cent of the drip interval. The stored information $I(k)$, initially about 6.8 bits, is seen to decrease, at first more rapid-

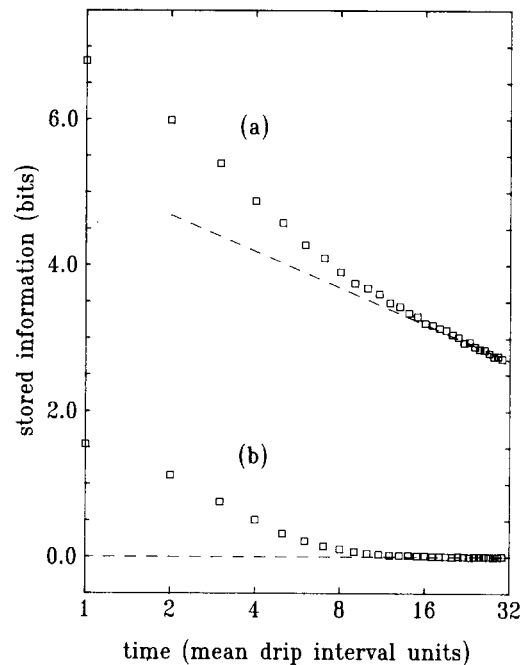


Fig. 4. Plots of stored information versus time. The time, which is expressed in multiples of the mean drip interval, is plotted on a logarithmic scale. Values of the stored information, which are computed from the data set of fig. 2d using eqs. (2) and (3), are indicated by the small squares. (a): The stored information $I(k)$ includes that associated with the phase variable. It decays from its initial value of 6.8 bits toward the dashed line, whose slope is -0.5 , the expected behavior when only phase information is present. (b): $I_1(k)$ includes only the information associated with the sequence of drip interval values, and decays toward zero as the drip intervals become uncorrelated.

ly, corresponding to the rapid loss of information associated with the chaotic behavior within the hump, and then more slowly, as the phase information is also lost, eventually decreasing like $-\log\sqrt{k}$, as expected for a purely stochastic drip sequence, $I_1(k)$ shows the stored information associated with the chaotic motion only, decaying smoothly from about 1.6 bits to zero after about 10 drip intervals. Thus we may characterize this attractor as possessing an information storage capacity of about 6.8 bits, of which about 5.2 bits are associated with the phase variable. Furthermore, the entropy generation rate is seen to be about 0.8 bits/drip, about half of which is associated with the phase variable. For the period-1 structure of fig. 2a, the information storage capacity, which is associated totally with the phase variable, is 8.3 bits, agreeing well with the observed (stochastic) scatter of 0.32 per cent of the drip interval. Correspondingly, the entropy generation rate here is only slightly less than its theoretical value of 0.5 bits/drip. As expected, $I_1(k)$ vanishes for this case. On the other hand, for the period-2 regime (fig. 2b), $I_1(k)$ remains at about 1 bit, and the information storage capacity is correspondingly greater. In general, for a period- n regime, $I_1(k) = \log_2(n)$ bits.

An interesting type of behavior is illustrated in figs. 2g, 2h. Attractors of this general form (the "eagle" in local parlance) appear over a fairly wide range of flow rates. Here, although the faucet is clearly in a chaotic regime, every other drip interval is nearly constant. This is seen by plotting the T_{n+2} versus T_n map for the "even" and "odd" drops, as shown in fig. 5 for the data of fig. 2g. One set of points yields a nearly periodic structure, while the other gives a chaotic attractor.

A consequence of this behavior is that one bit of information is propagated into the indefinite future, in the "phase" variable, indicating whether a particular drop interval is "even" or "odd". This is to be contrasted with the data set of fig. 2h, which, though similar in form, has a small cross-over region visible in the lower-left corner of the figure. This results in a small probability of "tunneling" between the even and odd phases, so that there is no long-term stored information. We do not yet completely understand the reasons underlying this phenomenon.

Further experimental work with the leaky faucet

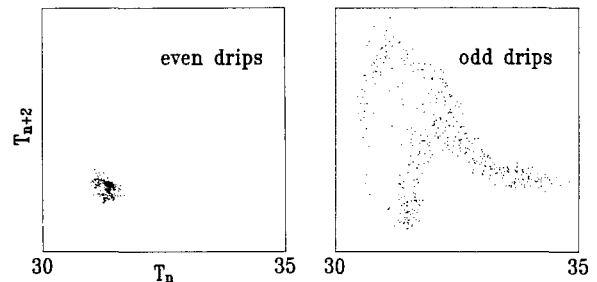


Fig. 5. T_{n+2} versus T_n return maps for the even and odd data points of fig. 2g.

system, perhaps taking additional system variables into account, is under contemplation. We also contemplate extending the application of information theory to other dynamical systems.

This research was supported by Faculty Research funds granted by the University of California, Santa Cruz. One of us (PLS) also gratefully acknowledges the recent hospitality of Professor Carson Jeffries and his research group at the University of California, Berkeley.

References

- [1] O. Rössler, in: *Synergetics: a workshop*, ed. H. Haken (Springer, Berlin, 1977) pp. 174–183.
- [2] R. Shaw, P. Martien and P. Scott, presented at the Order in chaos Conf. (Los Alamos, 1982); R. Shaw, presented at the Dynamic days Conf. (La Jolla, 1982).
- [3] P. Martien, An example of a chaotic attractor: the dripping faucet, UCSC Senior thesis in physics (1982); S. Pope, Information, chaos, and the kitchen sink, UCSC Senior thesis in physics (1984).
- [4] R. Shaw, *The dripping faucet as a model chaotic system* (Aerial Press, Box 1360, Santa Cruz, CA 95061).
- [5] C.E. Shannon and W. Weaver, *The mathematical theory of communication* (Univ. of Illinois Press, 1962).
- [6] D. Ruelle, *Ann. N.Y. Acad. Sci.* 316 (1978) 408; R.S. Shaw, *Z. Naturforsch.* 36a (1981) 80; J.P. Crutchfield and N.H. Packard, *Physica* 7D (1983) 201; K. Matsumoto and I. Tsuda, to be published.
- [7] A.N. Kolmogorov, *Dokl. Akad. Nauk SSSR* 124 (1959) 754; Y. Sinai, *Dokl. Akad. Nauk SSSR* 124 (1959) 768.